New Phytologist **Supporting Information Figs S1 & S2, Tables S1–S3 and Methods S1 & S2**

Article title: When do plant radiations influence community assembly? The importance of historical contingency in the race for niche space

Authors: Andrew J. Tanentzap, Angela J. Brandt, Rob D. Smissen, Peter B. Heenan, Tadashi Fukami, William G. Lee

Article acceptance date: 12 February 2015

The following Supporting Information is available for this article:

Fig. S1 Predicted vs observed mean annual air temperature (MAT) in the Murchison Mountains, South Island from 1982 to 2013.

Fig. S2 Schematic showing how niche occupancy can change over time.

Table S1 Sources of lineage ages

Table S2 Parameter estimates for model linking niche occupancy, diversification, and community dominance

Table S3 Molecular data used in genus-level phylogeny

Methods S1 Additional details and interpretation of palaeoreconstructions.

Methods S2 Estimation of phylogenetic hypothesis.

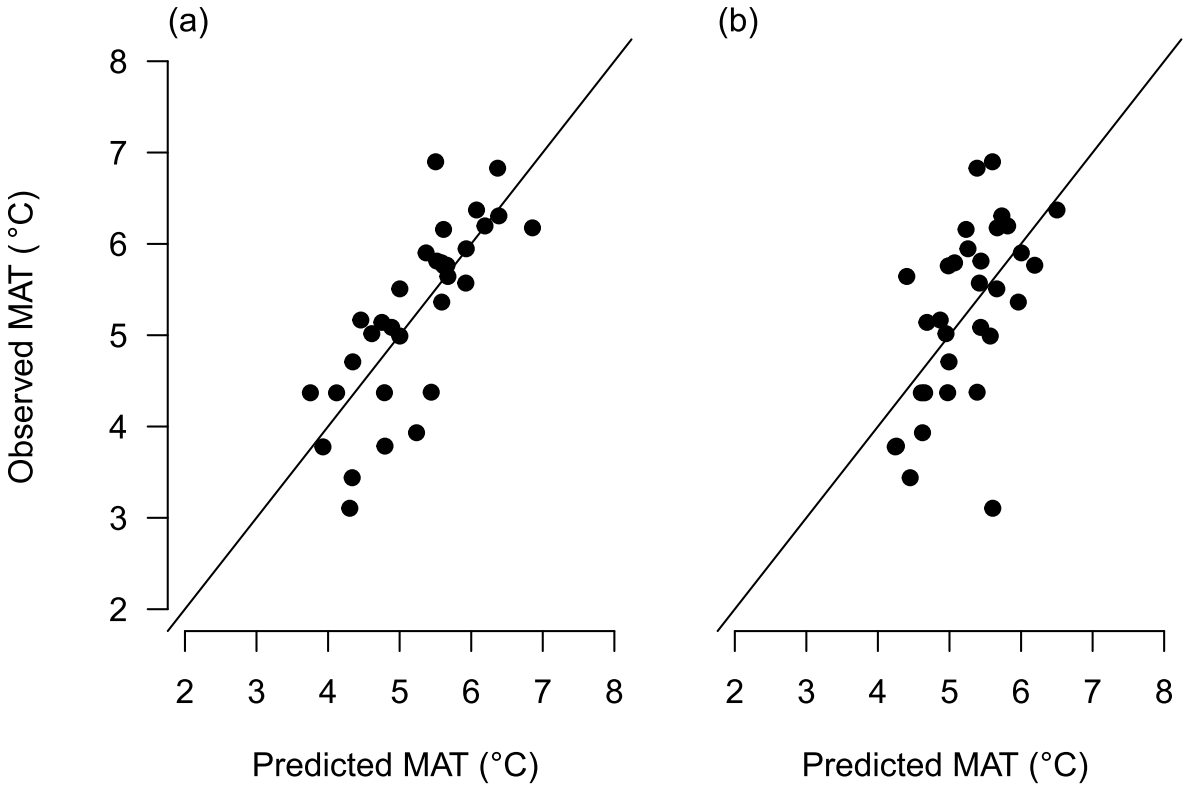

Fig. S1 Predicted vs observed mean annual air temperature (MAT) in the Murchison Mountains, South Island from 1982 to 2013. (a) Predicted MAT from sea surface temperature (SST) off Chatham Rise, whereby MAT = -21.73 + 1.76 SST; t_{30} = 6.90, P < 0.001 for effect of SST. (b) Predicted MAT from SST off South Tasman Rise, whereby MAT = -8.91 + 1.43SST; t_{30} = 3.93, P = 0.001 for effect of SST.

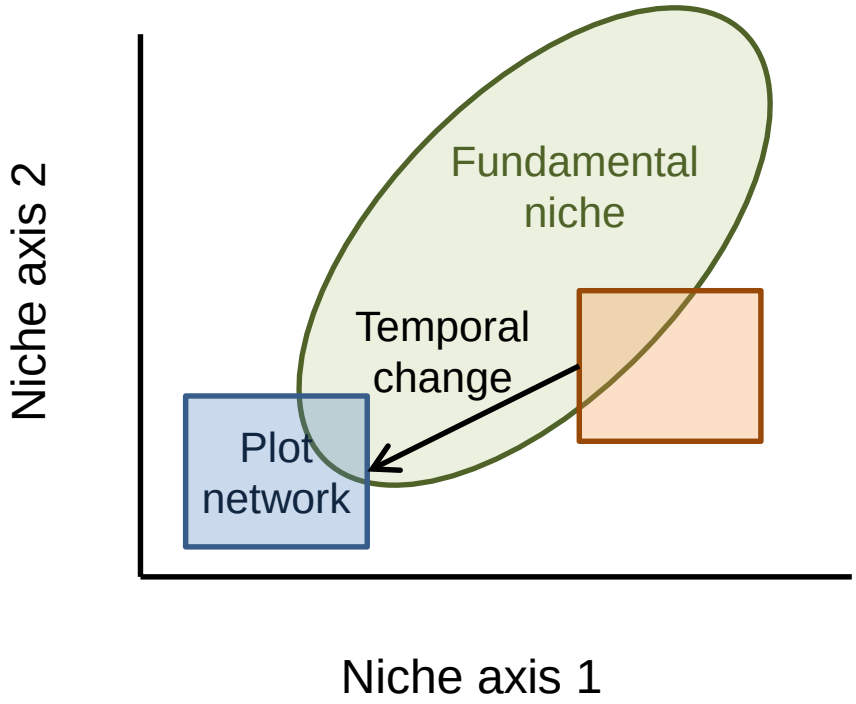

Fig. S2 Schematic showing how the niche occupancy of our plot network can change over time and overlap with different areas of a genus's fundamental niche. Estimating a genus's niche occupancy in this network solely from extant observations (e.g. blue square) may therefore lay well outside past climates (e.g. orange square). Considering a broader fundamental niche for each species corrects for this.

Table S1 References associated with each estimate of lineage age

Genus	Dating method	Genetic markers	References
Abrotanella	PL; BMCMC	*trn*K/*mat*K, ITS	Wagstaff *et al*. (2006); Swenson *et al*. (2012)
Aciphylla	BMCMC	ITS	Spalik *et al*. (2010)
Anisotome	BMCMC	ITS	Spalik *et al*. (2010)
Astelia	BMCMC	*trn*L, *pet*L−*psb*E, *psb*A−*trn*H, *trn*K−*rps*16, *NIA*-*i3*	Birch & Keeley (2013)
Chaerophyllum	BMCMC	ITS	Spalik *et al*. (2010)
Chionochloa	BMCMC	*trn*L−*trn*F, *rpl*16, *rbc*L, *ndh*F, *mat*K, *atp*B−*rbc*L, *trn*T−*trn*L, *trn*C−*trn*D, ITS, 26S rDNA; *trn*L−*trn*F, *rpl*16, *rbc*L, *ndh*F, *mat*K, *atp*B−*rbc*L, ITS, 26S rDNA	Antonelli *et al*. (2010); Pirie *et al*. (2012)
Craspedia	ML	*psb*A−*trn*H, ITS, ETS	Ford *et al*. (2007); K. A. Ford (pers. comm.)
Dracophyllum	PL, BMCMC	*rbc*L, *mat*K	Wagstaff *et al*. (2010)
Euphrasia	BMCMC	*atp*B−*rbc*L, *trn*L, *trn*L−*trn*F, ITS	Gussarova *et al*. (2008)
Forstera	ML	*rbc*L, ITS	Wagstaff & Wege (2002)
Gentianella	ML	ITS	von Hagen & Kadereit (2001)
Oreobolus	NPRS	ITS	Chacón *et al*. (2006)
Plantago	BMCMC	ITS	Tay *et al*. (2010)
Ranunculus	ML	ITS	Lockhart *et al*. (2001)

Veronica	ML	*rbc*L	Wagstaff *et al*. (2002)
Wahlenbergia	BMCMC	*trn*L−*trn*F, ITS	Prebble *et al*. (2011)

Studies estimated divergence times using either penalized likelihood (PL), mean path lengths/maximum likelihood (ML) methods, nonparametric rate smoothing (NPRS), or Bayesian MCMC sampling (BMCMC).

References

Antonelli A, Humphreys AM, Lee WG, Linder HP. 2010. Absence of mammals and the evolution of New Zealand grasses. *Proceedings of the Royal Society, B* **278:** 695−701.

Birch JL, Keeley SC. 2013. Dispersal pathways across the Pacific: the historical biogeography of *Astelia* s.l. (Asteliaceae, Asparagales). *Journal of Biogeography* **40:** 1914−1927.

Chacón J, Madriñán S, Chase MW, Bruhl JJ. 2006. Molecular phylogenetics of *Oreobolus* (Cyperaceae) and the origin and diversification of the American species. *Taxon* **55:** 359−366.

Ford KA, Ward JM, Smissen RD, Wagstaff SJ, Breitwieser I. 2007. Phylogeny and biogeography of *Craspedia* (Asteraceae: Gnaphalieae) based on ITS, ETS and *psb*A-*trn*H sequence data. *Taxon* **56:** 783−794.

Gussarova G, Popp M, Vitek E, Brochmann C. 2008. Molecular phylogeny and biogeography of the bipolar *Euphrasia* (Orobanchaceae): recent radiations in an old genus. *Molecular Phylogenetics and Evolution* **48:** 444−460.

von Hagen KB, Kadereit JW. 2001. The phylogeny of *Gentianella* (Gentianaceae) and its colonization of the southern hemisphere as revealed by nuclear and chloroplast DNA sequence variation. *Organisms, Diversity, and Evolution* **1:** 61−79.

Lockhart PJ, McLenachan PA, Havell D, Glenny D, Huson D, Jensen U. 2001. Phylogeny, radiation, and transoceanic dispersal of New Zealand alpine buttercups: molecular evidence under split decomposition. *Annals of the Missouri Botanical Garden* **88:** 458−477.

Pirie MD, Humphreys AM, Antonelli A, Galley C, Linder HP. 2012. Model uncertainty in ancestral area reconstruction: a parsimonious solution? *Taxon* **61:** 652−664.

Prebble JM, Cupido CN, Meudt HM, Garnock-Jones PJ. 2011. First phylogenetic and biogeographical study of the southern bluebells (*Wahlenbergia*, Campanulaceae).

Molecular Phylogenetics and Evolution **59:** 636−648.

Spalik K, Piwczyński M, Danderson CA, Kurzyna-Młynik R, Bone TS, Downie SR. 2010. Amphitropic amphiantarctic disjunctions in Apiaceae subfamily Apioideae. *Journal of Biogeography* **37:** 1977−1994.

Swenson U, Nylinder S, Wagstaff SJ. 2012. Are Asteraceae 1.5 billion years old? A reply to Heads. *Systematic Biology* **61:** 522−532.

Tay ML, Meudt HM, Garnock-Jones PL, Ritchie PA. 2010. DNA sequences from three genomes reveal multiple long-distance dispersals and non-monophyly of sections in Australasian *Plantago* (Plantaginaceae). *Australian Systematic Botany* **23:** 47−68.

Wagstaff SJ, Bayly MJ, Garnock-Jones PJ, Albach DC. 2002. Classification, origin, and diversification of the New Zealand *Hebes* (Scrophulariaceae). *Annals of the Missouri Botanical Garden* **89:** 38−63.

Wagstaff SJ, Breitwieser I, Swenson U. 2006. Origin and relationships of the austral genus *Abrotanella* (Asteraceae) inferred from DNA sequences. *Taxon* **55:** 95−106.

Wagstaff SJ, Dawson MI, Venter S, Munzinger J, Crayn DM, Steane DA, Lemson KL. 2010. Origin, diversification, and classification of the Australasian genus *Dracophyllum* (Richeeae, Ericaceae). *Annals of the Missouri Botanical Garden* **97:** 235−258.

Wagstaff SJ, Wege J. 2002. Patterns of diversification in New Zealand Stylidiaceae. *American Journal of Botany* **89:** 865−874.

Table S2 Species used in genus-level phylogeny and their associated accession numbers in GenBank for the *rbcL* gene region

Species	Genbank No.
Abrotanella linearifolia	JQ933200
Aciphylla aurea	JQ933204
Anisotome haastii	JQ933219
Astelia banksii	Y14983 A
Chaerophyllum temulum	JN891193
Chionochloa conspicua	HE573406
Craspedia incana	JQ933282
Dracophyllum acerosum	GQ392925
Euphrasia tetraquetra	N965543
Forstera tenella	AF451618
Gentianella propinqua	JN965557
Oreobolus pectinata	AF307927
Plantago major	JN965732
Ranunculus lyallii	EU053921
Veronica salicifolia	AF307921
Wahlenbergia angustifolia	EU713412

Table S3 Mean parameter estimates ± 95% credible intervals (CIs) for model linking niche occupancy, diversification, and community dominance (see Eqns 1–4)

Parameter	Mean	95% CIs
Regression coefficients		
Mean niche availability for genera with nonalpine ancestors and graminoid life forms ($\alpha^{(1)}$)	-0.92	-1.67 – -0.09
Effect of time on niche availability (β_1)	**0.34**	**0.11–0.57**
Effect of niche packing on niche availability (β_2)	0.12	-0.12–0.34
Change in niche availability with alpine ancestor ($\eta^{(1)}$)	0.11	-0.25–0.49
Change in niche availability with forb life form ($\gamma^{(1)}$)	0.06	-0.43–0.50
Change in niche availability with woody life form ($\gamma^{(1)}$)	0.09	-0.53–0.67
Mean species richness ($\alpha^{(2)}$; log-scale)	1.43	1.12–1.67
Effect of niche availability on species richness (β_3)	**0.54**	**0.24–0.93**
Effect of time independent of niche on species richness (β_4)	**0.27**	**0.02–0.50**
Effect of temporal variation in niche occupancy (β_5)	-0.16	-0.47–0.12
Effect of niche availability on arrival time (β_6)	2.00	1.59–2.23
Mean niche occupancy ($\alpha^{(3)}$)	-0.07	-0.18–0.06
Effect of species richness on niche occupancy (β_7)	**0.32**	**0.23–0.40**
Effect of arrival time on niche occupancy (β_8)	0.01	-0.07–0.11
Effect of plot frequency (β_9)	**0.18**	**0.09–0.27**
Mean generic abundance ($\alpha^{(4)}$)	-2.76	-2.98 – -2.52
Effect of occupancy on generic abundance (β_{10})	**0.68**	**0.61–0.76**
Change in generic abundance with alpine ancestor ($\eta^{(2)}$)	**0.74**	**0.56–0.93**
Change in generic abundance with forb life form ($\gamma^{(2)}$)	**-1.92**	**-2.15– -1.69**
Change in generic abundance with woody life form ($\gamma^{(2)}$)	**-1.82**	**-2.08– -1.56**
Mean generic richness	-2.81	-2.87 – -2.76
Effect of occupancy on generic richness	**0.15**	**0.12–0.17**
Effect of species richness on generic richness (β_{11})	0.01	-0.01–0.04
Change in generic richness with alpine ancestor	**0.13**	**0.09–0.17**
Change in generic richness with forb life form	**-0.15**	**-0.20 – -0.10**

Change in generic richness with woody life form	**-0.38**	**-0.43 – -0.34**
SD		
Residual variation in niche availability ($\sigma^{(1)}$)	0.16	0.05–0.39
Strength of residual phylogenetic variation in occupancy ($\sigma^{(2)}$)	1.13	0.93–1.42
Residual variation in generic abundance ($\sigma^{(3)}$; across all genera)	1.24	0.62–2.06
Variation in generic abundance among plots	0.19	0.07–0.31
Residual variation in generic richness	0.31	0.30–0.32
Variation in generic richness among plots	0.29	0.26–0.32

Methods S1 Additional details and interpretation of palaeoreconstructions.

Support for sea surface temperature (SST) reconstruction

We collated data from the only two core samples drilled in the Southwest Pacific by the Deep Sea Drilling Project (DSDP) and its successors to span both the Neogene and Quaternary, one from the cool-subtropical water of the Chatham Rise (site 593, 40°30′S, 167°40′E; Cooke *et al*., 2008) and the other from sub-Antarctic surface water of the South Tasman Rise (site 281, 40°30′S, 167°40′E; Shackleton & Kennett, 1975). For the Chatham Rise core, we obtained raw $\delta^{18}O : \delta^{16}O$ ratios relative to the Vienna Pee Dee Belemnite standard at different times for *Globigerina bulloides* and *Orbulina universa* (Cooke *et al*., 2008). These two species are planktonic foraminifera that reside in surface layers and for which the relationship between $\delta^{18}O$ in calcite and seawater has been extensively calibrated (Shackleton, 1974; Erez & Luz, 1983). Additionally, we used data on the extinct *Zeaglobigerina woodi*, as it was the only planktonic species found in the deeper parts of the core. Evidence suggests that *Zeaglobigerina woodi* resided in surface layers, though we excluded more recent samples from before the species became extinct (<14 million yr ago, Mya), as its depth stratification may have changed during this period (Cooke *et al*., 2008), and the isotopic record does not conform with the well-established enrichment of $\delta^{18}O$ in calcite arising from formation of the Antarctic ice sheets *c*. 12–14 Mya (Miller & Fairbanks, 1983; Zachos *et al*., 2001; but see Knorr & Lohmann, 2014). We then averaged measurements for multiple species at the same depth and calculated SST as:

$$SST = 16.998 - 4.52 \times (\delta^{18}O_{calcite} - \delta^{18}O_{seawater}) + 0.028 \times (\delta^{18}O_{calcite} - \delta^{18}O_{seawater})^2 \quad \text{Eqn S1}$$

where $\delta^{18}O_{seawater}$ was the Vienna Standard Mean Ocean Water from Table 6 of Cooke *et al*. (2008) and allowed to vary at different time intervals in relation to ice volume trends (values ranging between -0.83–0.39). Modern day predictions with $\delta^{18}O_{calcite} = 0.90$ and $\delta^{18}O_{seawater} = 0.39$ were lower than observed modern day SST by 0.65 so we applied this correction to the resulting values (Cooke *et al*., 2008). For the Tasman Ridge core, we similarly converted $\delta^{18}O$ measurements to SST using the methods described in Shackleton & Kennett (1975) and corrected for changes in ocean $\delta^{18}O$ composition as ice sheets formed using their Fig. 8. Samples were dated using age-depth data retrieved from the Ocean Drilling Program database

(www.odp.tamu.edu/database/). We excluded isotopic measurements from *Globorotalia miotumida*, as this species likely resided in deeper waters nearer to thermocline depth rather than exclusively in surface layers (Cooke *et al*., 2008).

Our interpretation of palaeo-SST is mostly confined to the Chatham Rise core because we found that annual means of modern SST inferred near this site by satellite measurements taken by the National Oceanic and Atmospheric Administration's Advanced Very High Resolution Radiometer were much more closely associated with MAT in the Murchison Mountains than those from the South Tasman Rise (R^2 = 0.60 and 0.32, respectively; Fig. S1). A model predicting MAT from both these cores was not a better fit to the data (R^2 = 0.61), and the effect of SST from the South Tasman Rise was no longer supported (mean effect ± SE = 0.46 ± 0.34, t_{29} = 1.34, P = 0.191 in model with both predictors; mean effect ± SE = 1.43 ± 0.36, t_{30} = 3.93, P = 0.001 from model only with this core; see Fig. S1 for Chatham Rise effects). Partly, this is unsurprising as the Murchison Mountains will be more strongly influenced by westerly winds that pass across the Tasman Sea and ocean temperatures in these warmer waters are not necessarily correlated with those in the sub-Antarctic (Pearson's correlation coefficient r = 0.59 between annual SST at the two core sites from 1982 to 2013). However, the two cores generally showed similar patterns with a few exceptions arising from their position in different oceanic waters.

Overall, the general trend of the two cores is consistent with observations elsewhere. First, we find clear evidence of a middle Miocene optimum around *c*. 15 Mya (Fig. 2). Although this yields similar temperatures to present day, the lack of topography in New Zealand would have meant that sites were much closer to sea level and thus considerably warmer. For example, a temperature of 5.5°C at 890 m above sea level (masl) would equate with nearly 13.5°C around 100 masl, and undoubtedly warmer temperatures further inland where New Zealand's rich fossil record has suggested MAT was between 15–22°C (Reichgelt *et al*., 2013; Pole, 2014). Moreover, the general finding that this period was warmer than present-day, as evidenced by warm temperate botanical elements (reviewed in Pole, 2014), may partly arise from geomorphological differences. Many of the Miocene plant macrofossils are found *c*. 300 masl, and MAT may have been at least 2°C warmer in these sites simply because of low topography. Second, we see consistent declines in temperature following formation of the Antarctic ice sheets *c*. 12–14 Mya (Fig. 2), leading to a Pliocene minimum. Finally, a general pattern of warming

follows, leading to peaks at between 3.0–3.5, 0.4–0.6 and 0.1 Mya, and a minimum at 0.95 Mya. This mirrors trends in glacial ice volume detected by natural gamma rays (Carter, 2005), as well as in isotopes to the east of South Island, where Quaternary changes in SST are strongly influenced by changes in the strength of sub-Antarctic inflows (Crundwell *et al*., 2008). Feary *et al*. (1991) detected strikingly similar patterns to ours around eastern Australia. They showed a sharp increase in SST through the Pliocene and throughout the Quaternary using a collection of 11 DSDP cores located between 15–55°S (Feary *et al*., 1991). Considerable variation in temperature is also a notable feature of the Quaternary (grey points, Fig. 2), likely associated with a period of relatively more dynamic changes in the volume of Antarctic ice sheets (Jouzel *et al*., 2007). For these reasons, a 25-point moving average fitted throughout the dataset is well justified.

Support for uplift reconstruction

Our elevation profile is generally consistent with detailed geomorphological studies. First, the start of uplift between 10–15 Mya predicted by (U-Th)/He ages is consistent with the age and rate of emergence of the Southern Alps. During this period, a change in the direction of the Pacific and Indo-Australian Plates produced a zone of convergence across the western length of South Island that gave rise to gradual topographic uplift (Kamp & Tippett, 1993; Sutherland *et al*., 2009). Second, damage trails detected in U fission fragments across more central and northerly parts of Southern Alps suggest that topography took an additional 1.3–3.7 million yr to form, during which the rate of denudation matched that of rock uplift (Tippett & Kamp, 1995). This was because uplift initially exposed soft sedimentary rocks that were easily eroded off the landscape (Tippett & Kamp, 1995). Consequently, mean surface elevation was near sea level in the late Miocene, as evident from stratigraphy around the margins of the Southern Alps (Kamp & Tippett, 1993). Third, analyses from across the Southern Alps suggest that uplift increased by an order of magnitude <1.3 Mya (Tippet & Kamp, 1993; Sutherland *et al*., 2009). While the absolute rate of uplift itself varies widely across the Southern Alps (Sutherland *et al*., 2009), the rate at which it has changed is likely to have been similar across the Murchison Mountains (Tippett & Kamp, 1995), supporting extrapolation across the range. Finally, we did not use dates derived from fission track analyses as elevation–age relationships may have been distorted by local geological processes (Sutherland *et al*., 2009), and previous work has only compared these

to average elevation within a surrounding 180 km^2 area (Tippett & Kamp, 1995), rather than the point from which samples were collected, as done here.

Plate tectonic changes have also shifted the Murchison Mountains by *c*. 3.4° latitude over the last 20 million yr (Nelson & Cooke, 2001), but we did not incorporate this into our temperature reconstructions. This is because the position of our primary sediment core has not moved further away relative to the Murchison Mountains over this period. Thus, the oceanic site from which we are relating SST to MAT on land has remained within cool-subtropical waters.

Assumptions of available niche space calculations

Implicitly, our approach assumes that the fundamental niches of ancestral species are conserved at the generic level over long periods of time. This is a reasonable first approximation for most of our study genera in the absence of past distributional data that we can use to assess niche stability (Nogués-Bravo, 2009), as almost all have dispersed wide distances (Winkworth *et al*., 2005), and may thus track climate more easily than adapt to new conditions (Holt & Gaines, 1992; Donoghue, 2008). Even if the niches that we inferred from GBIF data were truncated by biotic interactions, they generally exceeded the environmental space in our plot network, suggesting they could reliably be used to infer potential occupancy. All calculations of *E* involved genera with lower minimum DAT and DTC than that reconstructed in our plot network, and 75% of the calculations had genera with maximums exceeding that in our plots.

References

Carter RM. 2005. A New Zealand climatic template back to *c*. 3.9 Ma: ODP Site 1119, Canterbury Bight, South-West Pacific Ocean, and its relationship to onland successions. *Journal of the Royal Society of New Zealand* **35:** 9–42.

Cooke PJ, Nelson CS, Crundwell MP. 2008. Miocene isotope zones, paleotemperatures, and carbon maxima events at intermediate water-depth, Site 593, Southwest Pacific. *New Zealand Journal of Geology and Geophysics* **51:** 1–22.

Crundwell M, Scott G, Naish T, Carter L. 2008. Glacial–interglacial ocean climate variability from planktonic foraminifera during the Mid-Pleistocene transition in the temperate Southwest Pacific, ODP Site 1123. *Palaeogeography, Palaeoclimatology, Palaeoecology* **260:** 202–229.

Donoghue MJ. 2008. A phylogenetic perspective on the distribution of plant diversity. *Proceedings of the National Academy of Sciences, USA* **105:** 11549–11555.

Erez J, Luz B. 1983. Experimental paleotemperature equation for planktonic foraminifera. *Geochimica et Cosmochimica Acta* **47:** 1025–1031.

Feary DA, Davies PJ, Pigram CJ, Symonds PA. 1991. Climatic evolution and control on carbonate deposition in northeast Australia. *Palaeogeography, Palaeoclimatology, Palaeoecology* **89:** 341–361.

Holt RD, Gaines MS. 1992. Analysis of adaptation in heterogeneous landscapes: implications for the evolution of fundamental niches. *Evolutionary Ecology* **6:** 433–447.

Jouzel J, Masson-Delmotte V, Cattani O, Dreyfus G, Falourd S, Hoffmann G, Minster B, Nouet J, Barnola JM, Chappellaz J *et al.* 2007. Orbital and millennial antarctic climate variability over the past 800,000 years. *Science* **317:** 793–796.

Kamp PJJ, Tippett JM. 1993. Dynamics of Pacific plate crust in the South Island (New Zealand) zone of oblique continent–continent convergence. *Journal of Geophysical Research: Solid Earth* **98:** 16105–16118.

Knorr G, Lohmann G. 2014. Climate warming during Antarctic ice sheet expansion at the Middle Miocene transition. *Nature Geoscience* **7:** 376–381.

Miller KG, Fairbanks RG. 1983. Evidence for Oligocene–Middle Miocene abyssal circulation changes in the western North Atlantic. *Nature* **306:** 250–253.

Nelson CS, Cooke PJ. 2001. History of oceanic front development in the New Zealand sector of the Southern Ocean during the Cenozoic – a synthesis. *New Zealand Journal of Geology and Geophysics* **44:** 535–553.

Nogués-Bravo D. 2009. Predicting the past distribution of species climatic niches. *Global Ecology and Biogeography* **18:** 521–531.

Pole M. 2014. The Miocene climate in New Zealand: estimates from paleobotanical data. *Palaeontologia Electronica* **17:** 27A.

Reichgelt T, Kennedy EM, Mildenhall DC, Conran JG, Greenwood DR, Lee DE. 2013. Quantitative palaeoclimate estimates for Early Miocene southern New Zealand: evidence from Foulden Maar. *Palaeogeography, Palaeoclimatology, Palaeoecology* **378:** 36–44.

Shackleton NJ. 1974. Attainment of isotopic equilibrium between ocean water and the benthonic foraminifera genus *Uvigerina*: isotopic changes in the ocean during the last

glacial. In: Labeyrie L, ed. *Les méthodes quantitatives d'étude des variations du climat au cours du Pleistocène*. Paris, France: CNRS, 203–209.

Shackleton NJ, Kennett JP. 1975. Paleotemperature history of the Cenozoic and the initiation of Antarctic glaciation: oxygen and carbon isotope analyses in DSDP Sites 277, 279, and 281. *Initial reports of the Deep Sea Drilling Project* **29:** 743–755.

Sutherland R, Gurnis M, Kamp PJJ, House MA. 2009. Regional exhumation history of brittle crust during subduction initiation, Fiordland, Southwest New Zealand, and implications for thermochronologic sampling and analysis strategies. *Geosphere* **5:** 409–425.

Tippett JM, Kamp PJJ. 1993. Fission track analysis of the Late Cenozoic vertical kinematics of continental pacific crust, South Island, New Zealand. *Journal of Geophysical Research: Solid Earth* **98:** 16119–16148.

Tippett JM, Kamp PJJ. 1995. Quantitative relationships between uplift and relief parameters for the Southern Alps, New Zealand, as determined by fission track analysis. *Earth Surface Processes and Landforms* **20:** 153–175.

Winkworth RC, Wagstaff SJ, Glenny D, Lockhart PJ. 2005. Evolution of the New Zealand mountain flora: origins, diversification and dispersal. *Organisms Diversity & Evolution* **5:** 237–247.

Zachos J, Pagani M, Sloan L, Thomas E, Billups K. 2001. Trends, rhythms, and aberrations in global climate 65 Ma to present. *Science* **292:** 686–693.

Methods S2 Estimation of phylogenetic hypothesis.

We constructed a molecular-based phylogeny using representative species of our 16 genera. We first collated DNA sequences for the chloroplast marker *rbcL* from GenBank (http://www.ncbi.nih.gov; Table S3), and aligned these using MEGA 6 (Tamura *et al*., 2013). We then estimated tree structure and branch lengths using reversible-jump Markov chain Monte Carlo (MCMC) sampling in MrBayes v3.2 (Huelsenbeck *et al*., 2004). The best supported model of nucleotide substitution according was a General Time Reversible model with a proportion of invariable sites and gamma-distributed rate variation across sites (Nylander, 2004). We assumed that branch lengths were unconstrained (i.e. no molecular clock) and drew values from the default exponential prior with $\lambda = 10$ (Huelsenbeck *et al*, 2004). The topology of families and orders was constrained according to the APG III (2009) classification. Four independent Markov chains were estimated from two random starting points and run for 1,000,000 iterations, saving a total of 500 trees in the posterior sample. Chains converged within and between runs according to visual inspection of traces and standard diagnostics (potential scale reduction factor and deviation of the estimated posterior probability of splits in the tree).

References

Angiosperm Phylogeny Group (APG) III. 2009. An update of the Angiosperm Phylogeny Group classification for the orders and families of flowering plants: APG III. *Botanical Journal of the Linnean Society* **161:** 105–121.

Huelsenbeck JP, Larget B, Alfaro ME. 2004. Bayesian phylogenetic model selection using reversible jump Markov chain Monte Carlo. *Molecular Biology and Evolution* **21:** 1123–1133.

Nylander JAA. 2004. *MrModeltest v2. Software for comparing nucleotide substitution models*. [WWW document] URL http://www.abc.se/~nylander/mrmodeltest2/mrmodeltest2.html. [accessed 25 November 2014].

Tamura K, Stecher G, Peterson D, Filipski A, Kumar S. 2013. MEGA6: molecular evolutionary genetics analysis version 6.0. *Molecular Biology and Evolution* **30:** 2725–2729.